

Determination of minimum and maximum stress profiles using wellbore failure evidences: a case study—a deep oil well in the southwest of Iran

Abdollah Molaghab¹ · Mohammad Hossein Taherynia² · Seyed Mahmoud Fatemi Aghda² · Ahmad Fahimifar³

Received: 20 May 2016 / Accepted: 5 January 2017 / Published online: 24 January 2017
© The Author(s) 2017. This article is published with open access at Springerlink.com

Abstract The main objective of this paper is estimating the horizontal stresses and calibration of the log-derived horizontal stress profiles in deep oil wells according to their wall failure evidences, including both compressive (breakouts) and tensile failures (drilling-induced tensile fractures). Estimation of the horizontal stress profiles using well logs is one of the standard methods in the oil industry. Another method for estimating horizontal stresses is analyzing failure evidences in the wellbore wall. By integrating these two methods, a practical strategy was followed in this research to determine the horizontal stress profiles. By this strategy, minimum and maximum horizontal stress profiles are determined in such a way that the stress concentration at the wellbore wall at the tensile fracture identified depths, exceeds the formation tensile strength, while at the breakouts identified depths it exceeds the compressive strength of the formation. An advantage of this procedure is that does not require to measure in situ stresses. Also, due to the presence of a large number of breakouts and the induced fractures detected in different zones of a deep wellbore, log-derived stress profile calibration is done using the stress state in different zones that causes to increase the accuracy and reliability of the obtained horizontal stress profile. The proposed solution

was applied to determine the horizontal stress profiles in a deep oil well in the southwest of Iran as a real case.

Keywords Stress profile · Wellbore failure · Well logs · Formation strength · Tectonic strains

Introduction

Orientation and magnitude of principal stresses in hydrocarbon fields in are considered as a very important information in Petroleum Engineering. The stress state in the earth's crust controls stress concentration around a wellbore and therefore plays a critical role in wellbore instability, well stimulation operations, fluid flow in fractured reservoirs, and sand production (Bell 1996; Willson et al. 1999). Knowledge of the stress state is not only important in the petroleum industry, but it is also vital in geotechnical applications and other solid earth sciences. Thus, widespread studies have been conducted and different measurement methods and theories or empirical relationships have been established for estimating the stress state in the earth's crust. The underground stress state, with a simplifying assumption, can be described by three mutually orthogonal principal stress components, i.e., a vertical stress (S_v) and two horizontal principal stresses (S_H and S_h). S_v is a factor due to weight of the overburden, and its magnitude can be calculated using overburden density log (McGarr and Gay 1978). According to Zoback et al. (2003), hydraulic fracturing test, leak-off test (LOT), and measurement of pressure while drilling (PWD) are three common methods for the least principal stress measurement in the deep wells. The magnitude of minimum horizontal stress (S_h) in the normal and strike-slip faulting regimes can be measured using the mentioned methods. Measurement of the maximum horizontal stress (S_H) using the mentioned methods is not directly

✉ Seyed Mahmoud Fatemi Aghda
fatemi@khu.ac.ir

¹ Department of Geology, National Iranian South Oil Company, Ahwaz, Iran

² Department of Engineering Geology, Kharazmi University, Tehran, Iran

³ Department of Civil and Environmental Engineering, Amirkabir University of Technology, Tehran, Iran

possible (Zoback 2010) and is required to use theoretical and empirical relationships to estimate S_H based on S_h and S_v values (Binh et al. 2011; Zang et al. 2012). Also, other than being expensive and time-consuming, these tests cannot provide continuous horizontal stress profiles (Song and Hareland 2012; Sone and Zoback 2014). Therefore, development of the theoretical relationships for predicting stress state in deep oil wells is always of interest for the oil industry. In the following sections, first, the conventional techniques for determining horizontal stress profiles using the well logs are introduced. A discussion of the relationship between in situ stresses and wall rock strength at formation depths of break-outs and drilling-induced fractures will be given after that. Next, using a mathematically based strategy, the log-derived horizontal stress profiles are calibrated using in situ stress conditions that it can be estimated based on the observed wellbore wall failures at different depths. Finally, the horizontal stress profiles of a deep oil well in the southwest of Iran are determined using the introduced strategy and their results will be checked by analyzing compressive and tensile wellbore failures.

Determination of stress profiles using the well logs (log-derived stress profile)

One of the applicable methods for estimating horizontal stresses in the oil wells is to determine the stress profiles using acoustic and density logs (Blanton and Olson 1999). The key mechanical properties of wellbore wall rock for calculation of stress profiles based on the uniaxial strain theory, such as Poisson's ratio, overburden and pore pressure, can be determined using acoustic logs including compressional and shear wave velocities together with density log. The horizontal minimum stress profile of wellbores can be calculated using the proposed relationship based on the uniaxial strain theory, with inclusion of poroelasticity, as follows (Ahmed et al. 1991):

$$S_h = \frac{\nu}{1-\nu}(S_v - \alpha P_p) + \alpha P_p \quad (1)$$

where ν is Poisson's ratio, S_v is vertical total stress, α is Biot's poroelastic constant, and P_p is pore pressure.

The inconsistency of the horizontal stress profiles calculated from Eq. 1 with the horizontal stresses measured at different depths, necessitates applying some adjustments in Eq. 1 in order to improve its results. Tectonic stress is described by many investigators as one of the main reasons for the observed differences between calculated and measured horizontal stresses at different depths (Blanton and Olson 1999; Brown and Hoek 1978; Fjær et al. 2008; Zang et al. 2012; Zang and Stephansson 2008). Therefore, by adding the tectonic stress term, Eq. 1 is modified as follows (Hareland and Harikrishnan 1996):

$$S_h = \frac{\nu}{1-\nu}(S_v - \alpha P_p) + \alpha P_p + \sigma_{\text{tect}} \quad (2)$$

where σ_{tect} is calibration or additional tectonic stress.

By adding the tectonic stress term to Eq. 1, the horizontal stress profile can be displaced and its conformity with measured in situ stresses can be increased. The adding tectonic stress value is determined through difference between the measured value of stress at a specific depth and the stress calculated by Eq. 1 at the same depth.

Adding a constant value as tectonic stress to the calculated stress profile yields a good estimation of horizontal stress in sections of a wellbore that have the same lithology with the zone in which the in situ stress test has been carried out. It is worth mentioning that the wellbore wall is composed of layers with different lithology and elastic properties, it is a reasonable assumption that the tectonic stress will be varied in different lithological layers. To apply the tectonic stress, Blanton and Olson (1999) suggest assuming constant horizontal strains across all layers of a geological sequence with different elastic moduli. According to the study conducted by Blanton and Olson (1999), magnitude of the horizontal stresses can be computed using the following equations:

$$S_H = \frac{\nu}{1-\nu}(S_v - \alpha P_p) + \alpha P_p + \frac{E\varepsilon_x}{1-\nu^2} + \frac{\nu E\varepsilon_y}{1-\nu^2} + \frac{1+\nu E}{1-\nu^2}\alpha_t\Delta T \quad (3)$$

$$S_h = \frac{\nu}{1-\nu}(S_v - \alpha P_p) + \alpha P_p + \frac{E\varepsilon_y}{1-\nu^2} + \frac{\nu E\varepsilon_x}{1-\nu^2} + \frac{1+\nu E}{1-\nu^2}\alpha_t\Delta T \quad (4)$$

where ε_x and ε_y are tectonic strains in horizontal plane, E is the Young's modulus, α_t is thermal coefficient of expansion, and ΔT is temperature change (temperature at a particular depth minus the ambient surface temperature). Blanton and Olson (1999), for the sake of simplification, assumed that the horizontal strain in one direction is equal to zero (i.e., ε_x or $\varepsilon_y = 0$). In Eqs. 3 and 4 in addition to tectonic strain, the effect of temperature was considered in the calculation of horizontal stresses. There are two advantages in using the tectonic strain instead of the tectonic stress. The first one is to increase the accuracy of the minimum horizontal stress (S_h), and the second one is possibility of calculating the maximum horizontal stress (S_H) profile using well logs.

To achieve a log-derived stress profile with acceptable accuracy, at the least, the stress state in one point of well should be defined to calibrate the stress profile, which is required to carry out an in situ stress test in the well. Because the in situ stress measurement data are not available for many of deep oil wells, calibration of the log-derived horizontal stress profile, and reaching to a reliable

estimation of the horizontal stress values are not possible for all drilled wells.

Wellbore failures analysis

Analyzing failures of the wellbore wall, which can be detected using wellbore imaging devices, provides valuable information about the stress state at deep wells (Zoback et al. 2010). Generally, considering the condition of stress concentration around a wellbore, there are possibility of occurrence of compressive failures (breakouts) and/or tensile failures (drilling-induced tensile fractures) in the wellbore wall (Gough and Bell 1981, 1982). Stress concentration around the wellbore drilled in a stressed elastic medium can be calculated using equations developed by Kirsch (1898). Considering the assignability of the stress concentration and the nature of the created failures at the wellbore wall, it is possible to extract useful information about in situ stress magnitudes utilizing a suitable failure criterion (Zoback et al. 2003). The Mohr–Coulomb and maximum tensile stress criteria are the most commonly used failure criteria for analysis of shear failure and tensile failure, respectively (Rasouli et al. 2011). Zoback et al. (2003) presented a simple strategy for estimation of horizontal stress state in deep wellbores based on the failure evidences of wellbore wall and tectonic regime of the studied field. In this method, the allowable values of horizontal stresses, which are illustrated in a stress polygon, is obtained using the friction coefficient of the earth’s crust as follows (Jaeger and Cook 1979):

$$\frac{S_1 - P_P}{S_3 - P_P} \leq \left[(\mu^2 + 1)^{1/2} + \mu \right]^2 \tag{5}$$

where μ is the coefficient of frictional sliding on an optimally oriented pre-existing fault. S_1 and S_3 are the maximum and minimum principal stresses which can be corresponded to S_H , S_h , or S_v using Anderson’s faulting theory. Then, the range of allowable values of horizontal stresses is limited based on non-catastrophic failures of the wellbore with respect to the rock strength of the wellbore wall. The most common non-catastrophic borehole failures are breakouts that formation will be lead to enlargement of the wellbore cross section (Bell and Gough 1979). The enlargement of the wellbore is caused by the development of intersecting conjugate shear planes, which cause pieces of the borehole wall to spall off (Reinecker et al. 2003). Therefore, breakouts can be detected using the (four-arm) caliper log tool that provides two diameters of the borehole cross section (Reinecker et al. 2003). The Formation mechanism of the breakout was first discussed by Gough and Bell (1981) and later expanded by Zoback et al. (1985). Breakouts are

formed in symmetric zones around the borehole at the azimuth of least horizontal principal stress ($\theta = 90^\circ, 270^\circ$) where the circumferential stress ($\sigma_{\theta\theta}$) is the largest and exceeds the formation compressive strength.

$$\sigma_{\theta\theta}^{\max} \geq (UCS + N\phi \times \Delta P) \tag{6}$$

where UCS is the uniaxial compressive strength, ΔP is the difference between the wellbore pressure (mud weight, P_m) and pore pressure (P_P), and $N\phi$ is calculated using rock friction angle (ϕ).

$$N\phi = \frac{1 + \sin \phi}{1 - \sin \phi} \tag{7}$$

Based on Kirsch’s equations, the maximum values of $\sigma_{\theta\theta}$ can be calculated as:

$$\sigma_{\theta\theta}^{\max} = 3S_H - S_h - 2P_P - \Delta P - \sigma^{\Delta T} \tag{8}$$

where $\sigma^{\Delta T}$ represents the thermal stresses arising from the difference between the mud temperature and formation temperature (ΔT), and ΔP is the difference between the wellbore pressure (mud weight, P_m) and pore pressure (P_P).

Drilling-induced fractures are another common wellbore failure that appeared as two narrow sharply defined fractures formed on two opposite sides of the wellbore wall. These longitudinal fractures are sub-parallel or slightly inclined to the wellbores axis in vertical wells (Tingay et al. 2008). Drilling-induced tensile fractures are created when the circumferential stress ($\sigma_{\theta\theta}$) is negative and exceeds the tensile strength (T_0) of the formation (Aadnoy 1990):

$$\sigma_{\theta\theta}^{\min} \leq -T_0 \tag{9}$$

Based on Kirsch’s equations, the circumferential stress ($\sigma_{\theta\theta}$) around a vertical borehole is minimum in the S_H direction ($\theta = 0, 180$) and can be calculated as:

$$\sigma_{\theta\theta}^{\min} = 3S_h - S_H - 2P_P - \Delta P - \sigma^{\Delta T} \tag{10}$$

Calibration of log-derived stress profiles using wellbore failure evidences

For estimating the maximum and minimum horizontal stresses, both mentioned methods have some limitations in practice. Determining the log-derived stress profiles using Blanton and Olson (1999) method (Eqs. 3, 4) the stress state must be known in a depth of the well that is not available for many deep oil wells. Also, for determination of a particular range of horizontal stresses using analysis of the wellbore failure evidences, both breakout and induced tensile fracture must be available at the same depth of the wellbore. Thus, application of this method becomes limited, as in many cases, the breakouts and induced tensile fractures are not formed at same depths.

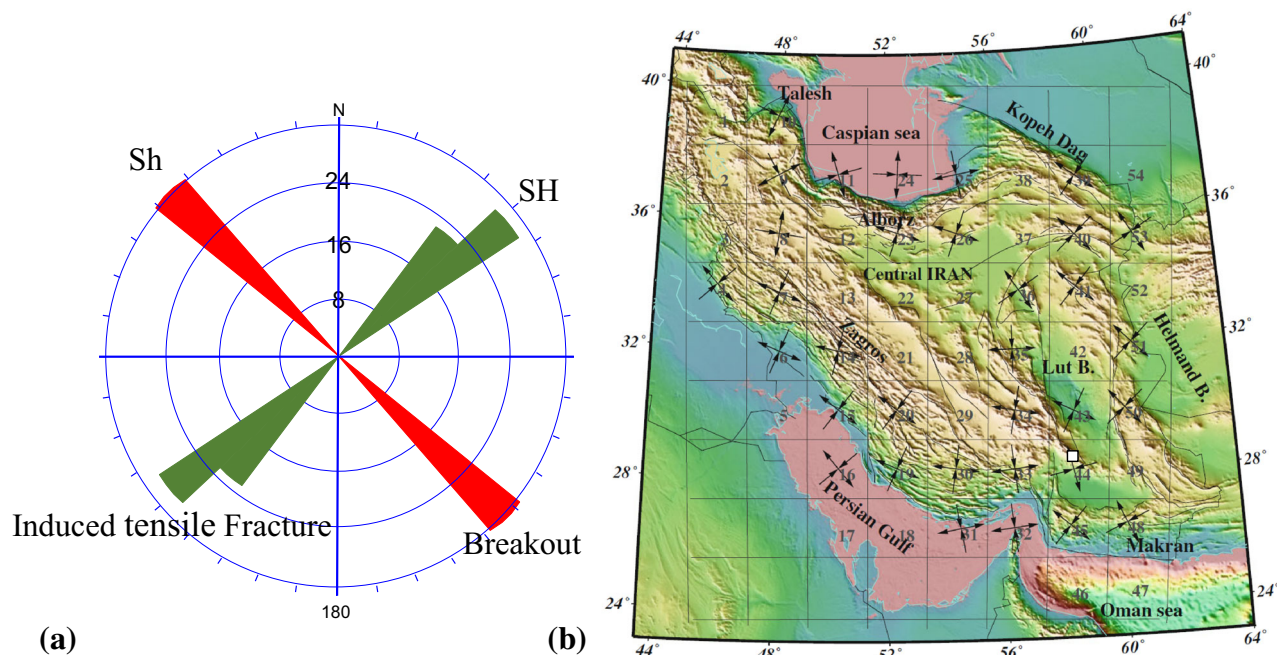


Fig. 1 **a** Azimuth of horizontal stresses based on orientation of wellbore failures in the studied well, **b** Map of maximum and minimum horizontal stress orientations in Iran (Zarifi et al. 2013)

However, the failure evidences at different depths of a wellbore can be used for calibration of the horizontal stress profiles. In this strategy, the stress condition in formation zones of breakouts and induced tensile fractures at different depths of a wellbore are related using Eqs. 3 and 4. By replacing S_h and S_H in Eqs. 8 and 10 that, respectively, the stress condition required to form the breakout and induced tensile fractures by the equal defined terms from Eqs. 3 and 4, Eqs. 11 and 12 can be obtained as:

$$\frac{E\varepsilon_x}{1-\nu^2}(3-\nu) + \frac{E\varepsilon_y}{1-\nu^2}(3\nu-1) + 2S_h - p_f - p_{mw} - USC - N\phi \times \Delta P \geq 0 \quad (11)$$

$$\frac{E\varepsilon_y}{1-\nu^2}(3-\nu) + \frac{E\varepsilon_x}{1-\nu^2}(3\nu-1) + 2S_h - p_f - p_{mw} - \sigma^{\Delta T} + T_0 \leq 0 \quad (12)$$

where S_h is the horizontal stress arising from the overbidding loading that is calculated using Eq. 1.

To solve Eqs. 11 and 12, they must be assumed equal to zero or equal to a certain amount. Breakout incidence in a wellbore wall indicates that Eq. 11 is equal or greater than zero. Also, the occurrence of induced fracture suggests that Eq. 12 is equal or less than zero. These equations can be considered approximately equal to zero at both end points of breakouts and induced fractures. Therefore, the data obtained from these points are used for solving Eqs. 11 and 12. Hence, in Eqs. 11 and 12, tectonic strain parameters of ε_x and ε_y are

the only unknown, using two calibration points, these equations will be solved and these two unknown parameters can be determined. With replacing elastic properties of the wall rock and the other parameters for each end point of a wellbore failure, an equation will be obtained. However, considering the inaccuracies and errors in involved data, the use of more calibration points can be caused to increase the accuracy level of the results. In many cases, there are several breakouts and induced fractures at different depths of a wellbore and, therefore, more than two equations can be obtained. Hence, to improve the accuracy level of the estimated tectonic strain parameters, the least-squares approach was used in this study.

Applications and validation of the results

The proposed approach was used to estimate the horizontal stresses in a deep wellbore in an oil field located in southwest of Iran. The depth of the studied wellbore is about 4200 m and data obtained from 360 m intervals between 3800 m to 4160 m. By using full-bore formation microimager (FMI) and caliper logs, several induced fractures and breakouts were detected in the studied interval. Azimuth of the maximum and minimum horizontal stresses were established based on the orientation of breakouts and induced fractures in the studied wellbore as shown in Fig. 1a. Moreover, Fig. 1b illustrates the maximum and minimum horizontal stress orientations in Iran.

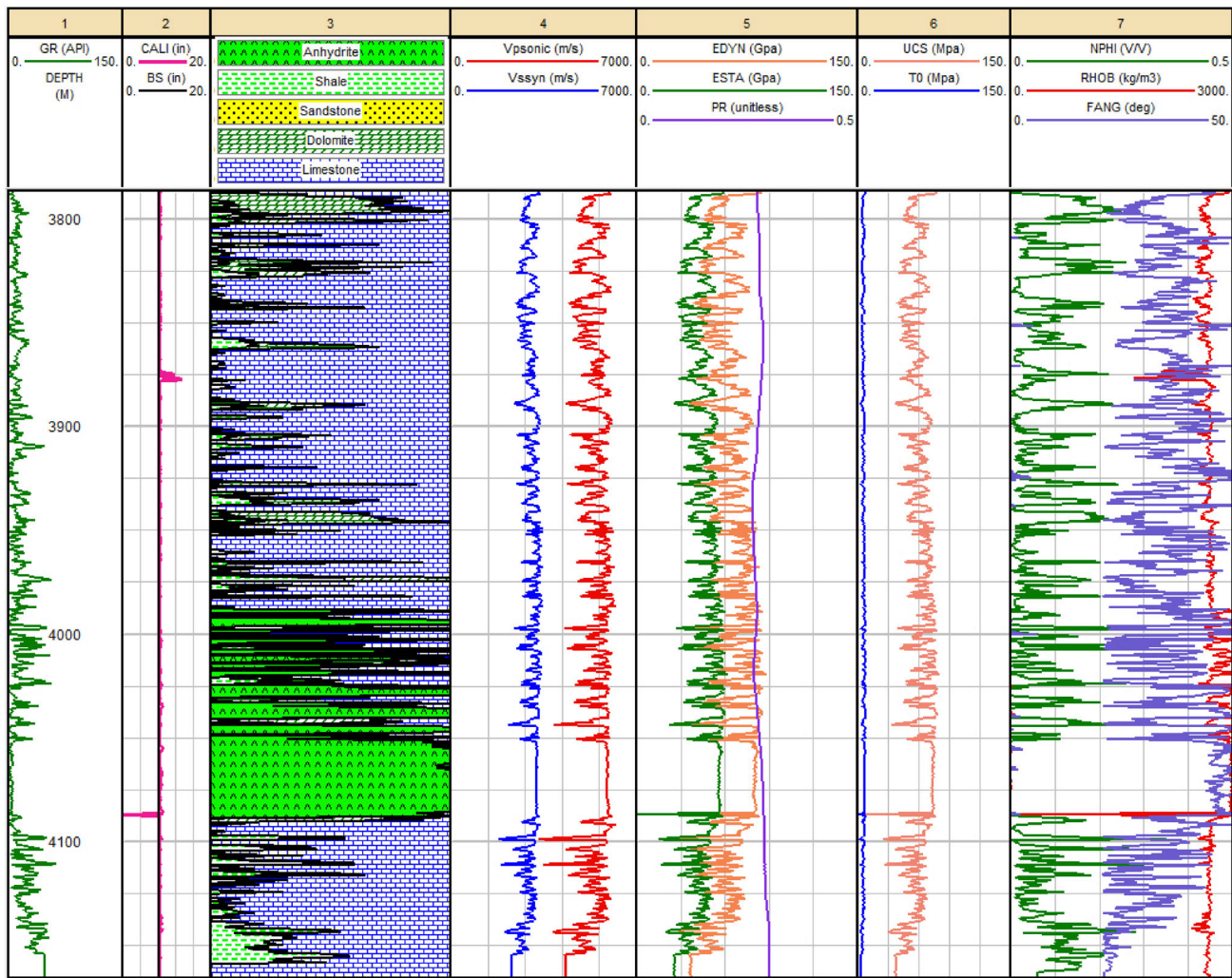


Fig. 2 Logs of elastic moduli (Young’s modulus, Poisson ratio) and strength parameters (UCS, T_0 , and $N\phi$) for the studied interval

As shown in Fig. 1, the orientation of borehole breakouts that indicate azimuth of S_h is about 43° and the orientation of induced fractures that indicate azimuth of S_H is about 133° .

Using acoustic (ΔTS and ΔTC) and density logs (Fig. 2), the required parameters to solve Eqs. 11 and 12 were determined. Furthermore, using FMI images, the end points of breakouts and the induced fractures were selected as calibration points.

Using FMI images, 24 points, i.e., 12 breakouts and 12 induced fractures, were selected in the studied interval. On the basis of the proposed solution, the optimum values for ϵ_x and ϵ_y (two unknown parameters) with a minimum error in these 24 points are $5.1e-4$ and $-6.8e-4$, respectively.

Based on the estimated tectonic strain parameters, the maximum and minimum horizontal stresses were calculated using Eqs. 3 and 4, and the vertical stress was calculated by integration of density logs. The obtained results are shown in Fig. 3.

The circumferential effective stress around the wellbore ($\sigma_{\theta\theta}$) and the strength of the wall rock at different parts of a breakout and an induced fracture in the selected interval of the wellbore are shown in Fig. 4. In both ends of the breakout and the induced fractures, the circumferential effective stress is almost equal to the formation strength. However, at the mid points of the breakout and the induced fractures, the circumferential effective stress is exceeded the formation strength.

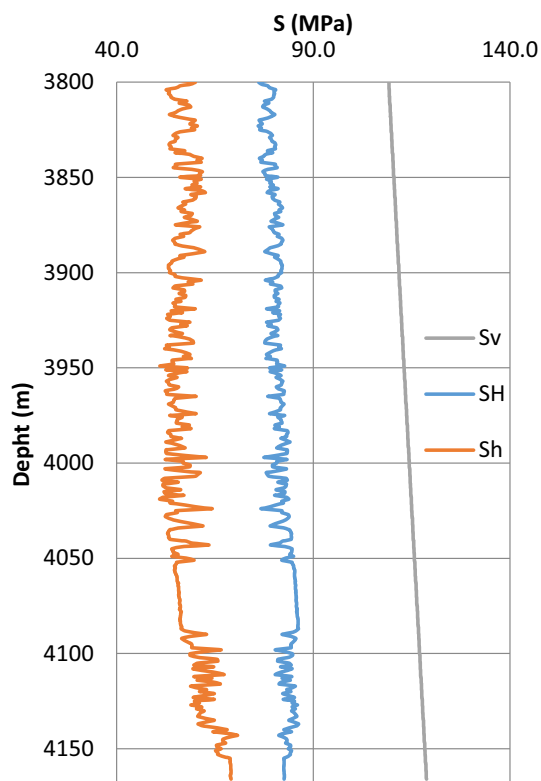


Fig. 3 Estimated three principal stress profile in the studied interval

Through some laboratory experiments, Zoback et al. (1985) observed that after initial formation of a breakout, the stress concentration around the wellbore is such that the breakout tends to deepen while the breakout width remains constant. The following equation was developed by Barton et al. (1988) to estimate in situ horizontal stresses using breakout width (W_{bo}):

$$S_H = \frac{(USC + 2P_p + \Delta P + \sigma^{\Delta T}) - S_h(1 + 2 \cos 2\theta_b)}{1 - 2 \cos 2\theta_b} \quad (13)$$

where $2\theta_b = \pi - W_{bo}$.

Figure 5 shows the possible stress state polygon, at depth of 4143 m which is constrained by frictional coefficients 0.6–0.8 that are common values for μ (Handin 1969; Nelson et al. 2005). FMI images of the studied well indicate the presence of a breakout with an average width of 46° at depth of 4143 m, but there is not induced fracture in this depth. The possible stress ranges in the absence or presence of induced fracture (dash line) are shown in Fig. 5. The dash-dot line shows the magnitude of S_H (for a given value of S_h) that is required to cause breakouts with a

width of 46° ($\theta = 67$) by using Eq. 13 and considering $P_p = 47$ MPa, $\Delta P = 3.8$ MPa, and $USC = 75.9$ MPa. The effect of wellbore cooling was disregarded, because there was no significant temperature difference between the drilling mud and the formation in the studied interval. However, as stated by Zoback et al. (2003), even for the large temperature differences (ΔT) such as 25°C , significant changes do not exert on the estimated stresses.

As shown in Fig. 5, the horizontal stresses derived from the calibrated stress profile at the mentioned depth, fall within the possible range of stresses (see study carried out by Zoback et al. 2003).

Furthermore, in order to check the accuracy level of the obtained log-derived stress profiles, Eq. (13) was rewritten in the following form to determine the breakout width using the magnitude of the horizontal stresses:

$$\frac{S_h + S_H - P_p - \Delta P - \sigma^{\Delta T} - USC}{2(S_H - S_h)} = \cos 2\theta. \quad (14)$$

A comparison between the changes of breakout widths obtained by Eq. 14 and the breakout widths in the FMI images at two different intervals can be seen in Fig. 6.

As displayed in Fig. 6, there is an acceptable compliance between the calculated and the actual breakout widths that indicates accuracy level of the estimated horizontal stresses.

Conclusions

In this research, a practical strategy for calibration of the log-derived stress profile using failure evidences of the wells was developed. In this strategy, as discussed earlier, the minimum and maximum horizontal stress profiles were determined. In the proposed approach, values of two tectonic strains in horizontal plane (ε_x and ε_y) used for calibration of log-derived stress profiles are assumed constant in the studied interval and are determined based on stress conditions in the detected failure evidence at the wellbore wall. Therefore, using this strategy, the magnitude of tectonic strain in two directions (ε_x and ε_y) can be determined, and it is not required to consider one of these parameters equal to zero. Considering the proposed method, the maximum and minimum horizontal stress profiles of a deep oil well in the southwest of Iran were calibrated based on wellbore failure evidences detected at different depths. Comparing the obtained values of horizontal stresses at various depths of the studied interval using this method and other techniques indicates the reliability of the estimated

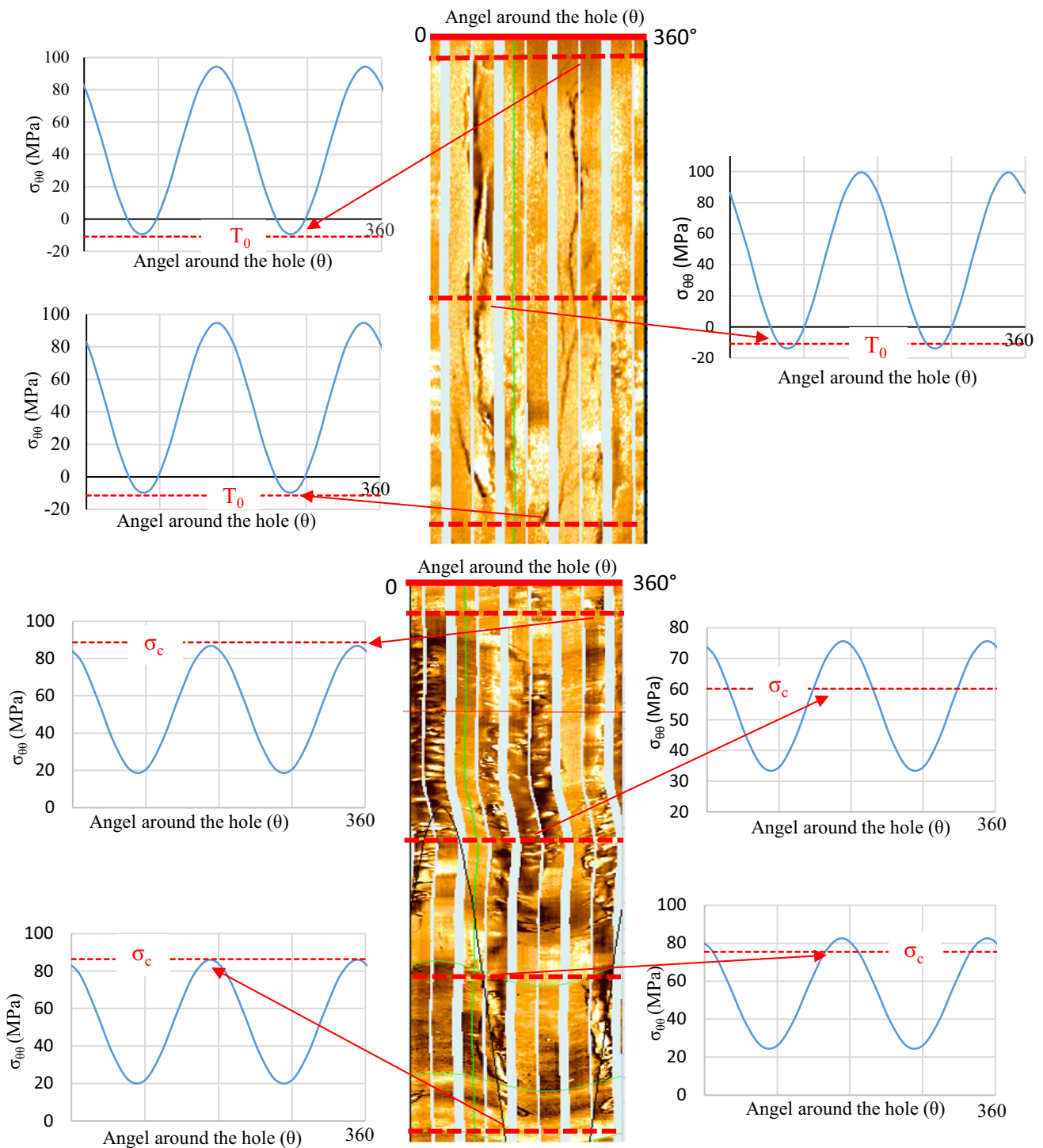


Fig. 4 The circumferential effective stress ($\sigma_{\theta\theta}$) and the strength of formation (*horizontal dash line*) in different parts of the indicated breakout and induced fracture in the studied interval

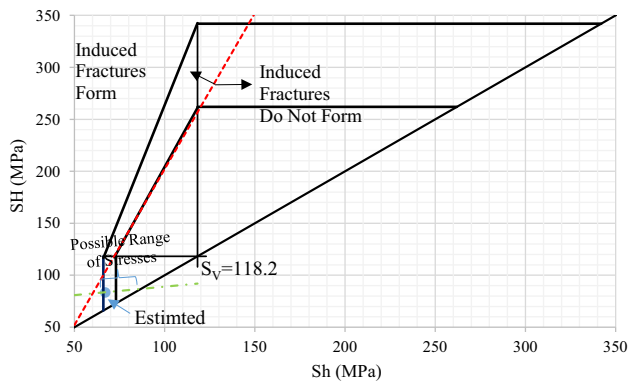


Fig. 5 Stress polygon that define possible magnitudes of S_h and S_H at the depth of 4143 m. *Dash line* represent the stress condition of occurring or do not occurring of induced tensile fracture and *dash-dot line* represent the required stress condition for forming of breakout with $W_{bo} = 46^\circ$. *Blue point* indicates horizontal stresses at the depth 4143 m based on the log-derived stress profile



Fig. 6 Compression of calculated (*dash line*) and observed breakout widths in different depths of the wellbore

stress profiles. The proposed technique in this study can be used in the other projects with similar conditions.

Acknowledgements The authors would like to express their appreciation to the National Iranian South Oil company for providing filed data and also permission of using data. Moreover, the authors really appreciate Dr. A. Moradi and Dr. Armaghani for his technical help and advice.

Open Access This article is distributed under the terms of the Creative Commons Attribution 4.0 International License (<http://creativecommons.org/licenses/by/4.0/>), which permits unrestricted use, distribution, and reproduction in any medium, provided you give appropriate credit to the original author(s) and the source, provide a

link to the Creative Commons license, and indicate if changes were made.

References

- Aadnoy BS (1990) Inversion technique to determine the in situ stress field from fracturing data. *J Pet Sci Eng* 4:127–141
- Ahmed U, Markley ME, Crary SF (1991) Enhanced in-situ stress profiling with microfracture, core, and sonic-logging data. *SPE Form Eval* 6(02):243–251
- Barton CA, Zoback MD, Burns KL (1988) In-situ stress orientation and magnitude at the Fenton Geothermal Site, New Mexico, determined from wellbore breakouts. *Geophys Res Lett* 15(5):467–470
- Bell JS (1996) Petro geoscience 2. In situ stresses in sedimentary rocks (part 2): applications of stress measurements. *Geosci Can* 23(3):135–153
- Bell J, Gough D (1979) Northeast-southwest compressive stress in Alberta evidence from oil wells. *Earth Planet Sci Lett* 45:475–482
- Binh NTT, Tokunaga T, Gouly NR, Son HP, Van Binh M (2011) Stress state in the Cuu Long and Nam Con Son basins, offshore Vietnam. *Mar Petrol Geol* 28:973–979
- Blanton TL, Olson JE (1999) Stress magnitudes from logs: effects of tectonic strains and temperature. *SPE Reserv Eval Eng* 2(1):62–68
- Brown E, Hoek E (1978) Trends in relationships between measured in situ stresses and depth. *Int J Rock Mech Min Sci Geomech Abstr* 15:211–215
- Fjær E, Holt R, Horsrud P, Raaen A, Risnes R (2008) *Petroleum Related Rock Mechanics*. Development in Petroleum Science vol 33. Elsevier Science Publishers B.V, Amsterdam
- Gough D, Bell J (1981) Stress orientations from oil-well fractures in Alberta and Texas. *Can J Earth Sci* 18:638–645
- Gough D, Bell J (1982) Stress orientations from borehole wall fractures with examples from Colorado, east Texas, and northern Canada. *Can J Earth Sci* 19:1358–1370
- Handin J (1969) On the Coulomb–Mohr failure criterion. *J Geophys Res* 74:5343–5348
- Hareland G, Harikrishnan R (1996) Comparison and verification of electric-log-derived rock stresses and rock stresses determined from the Mohr failure envelope. *SPE Form Eval* 11:219–222
- Jaeger JC, Cook NGW (1979) *Fundamentals of rock mechanics*. Chapman and Hall, London
- Kirsch G (1898) *Die Theorie der Elastizität und die Bedürfnisse der Festigkeitslehre*. Springer, Berlin
- McGarr A, Gay N (1978) State of stress in the earth's crust. *Annu Rev Earth and Planet Sci* 6:405
- Nelson EJ, Meyer JJ, Hillis RR, Mildren SD (2005) Transverse drilling-induced tensile fractures in the West Tuna area, Gippsland Basin, Australia: implications for the in situ stress regime. *Int J Rock Mech Min Sci* 42:361–371
- Rasouli V, Pallikathakathil ZJ, Mawuli E (2011) The influence of perturbed stresses near faults on drilling strategy: a case study in Blacktip field North Australia. *J Petrol Sci Eng* 76:37–50
- Reinecker J, Tingay M, Müller B (2003) Borehole breakout analysis from four-arm caliper logs. *World Stress Map Project*:1–5
- Sone H, Zoback MD (2014) Viscous relaxation model for predicting least principal stress magnitudes in sedimentary rocks. *J Petrol Sci Eng* 124:416–431
- Song L, Hareland G (2012) Minimum horizontal stress profile from logging data for montney formation of North East British Columbia. In: *SPE-162233-MS* presented at SPE Canadian

- Unconventional Resources Conference, Calgary, Alberta, Canada (30 Oct–1 Nov 2012)
- Tingay M, Reinecker J, Müller B (2008) Borehole breakout and drilling-induced fracture analysis from image logs. World Stress Map Project Stress Analysis Guidelines 1–8
- Willson S, Last N, Zoback M, Moos D (1999) Drilling in South America: a wellbore stability approach for complex geologic conditions. In: SPE-53940-MS presented at Latin American and Caribbean Petroleum Engineering Conference, Caracas, Venezuela (21–23 April 1999)
- Zang AHW, Stephansson OJ (2008) Stress field of the earth's crust. Springer, Netherlands
- Zang A, Stephansson O, Heidbach O, Janouschkowitz S (2012) World stress map database as a resource for rock mechanics and rock engineering. *Geotech Geol Eng* 30:625–646
- Zarifi Z, Nilfouroushan F, Raeesi M (2013) Crustal stress map of Iran: insight from seismic and geodetic computations. *Pure Appl Geophys* 171(7):1219–1236
- Zoback MD (2010) Reservoir geomechanics. Cambridge University Press, Cambridge
- Zoback MD, Moos D, Mastin L, Anderson RN (1985) Well bore breakouts and in situ stress. *J Geophys Res Solid Earth* 90:5523–5530
- Zoback MD et al (2003) Determination of stress orientation and magnitude in deep wells. *Int J Rock Mech Min Sci* 40(7–8):1049–1076
- Zoback MD, Paul P, Lucier A (2010) Utilizing observations of borehole failure in deviated wellbores to constrain the full stress tensor in deep wells and mines: application to two complex case studies. Presented at International Symposium on in-situ Rock Stress, Beijing, China, (25–27 August 2010):69–76